

Fluorinated diamondlike carbon templates for high resolution nanoimprint lithography

M. Schwartzman

*Department of Chemical Engineering, Columbia University, New York, New York 10027
and The Nanotechnology Center for Mechanics in Regenerative Medicine, Columbia University,
New York, New York 10027*

A. Mathur and Y. Kang

*Department of Mechanical Engineering, Columbia University, New York, New York 10027
and The Nanotechnology Center for Mechanics in Regenerative Medicine, Columbia University,
New York, New York 10027*

C. Jahnes

IBM, T. J. Watson Research Center, Yorktown Heights, New York 10598

J. Hone

*Department of Mechanical Engineering, Columbia University, New York, New York 10027
and The Nanotechnology Center for Mechanics in Regenerative Medicine, Columbia University,
New York, New York 10027*

S. J. Wind^{a)}

*Department of Applied Physics and Applied Mathematics, Columbia University, New York, New York 10027
and The Nanotechnology Center for Mechanics in Regenerative Medicine, Columbia University,
New York, New York 10027*

(Received 7 July 2008; accepted 7 October 2008; published 1 December 2008)

Nanoimprint templates were fabricated from diamondlike carbon (DLC) films grown on Si, using negative-tone e-beam lithography and oxygen plasma etching. An antiadhesion coating was provided through fluorocarbon-based plasma treatment, which was found to form a Teflon-like thin layer on the treated DLC surface. The fluorinated templates were used to imprint arrays of dots with diameters down to 10 nm in polymethyl-methacrylate. Application of the fluorocarbon plasma treatment was also demonstrated in the antiadhesion treatment of the nanoimprint resist and in elastomer molding. © 2008 American Vacuum Society. [DOI: 10.1116/1.3013281]

I. INTRODUCTION

Since the introduction of nanoimprint lithography,¹ silicon,^{2,3} quartz,⁴ and silicon dioxide^{5,6} have been the most commonly used materials for nanoimprint templates. Alternative materials, such as silicon carbide⁷ and diamond,^{8–10} have been reported, but they have not yet seen widespread use.

One of the most critical aspects of the nanoimprint lithography (NIL) process is the separation of the template from the imprinted surface at the end of the imprint. Ideally, the template surface should be left clean of any resist residue and ready for the next imprint cycle, while the imprinted resist should be free of damage while maintaining adhesion to the substrate. Neglecting the case of cohesive failure in the bulk of the imprinted resist during the separation, which would leave polymer residuals both on the imprinted substrate and on the template, this scenario can be achieved by strengthening the adhesion between the polymer to the imprinted substrate, as well as by weakening the adhesion between the polymer and the template. In addition, weak adhesion between the template and the resist will promote easy separation without the application of significant mechanical force. In order to achieve this goal, the template surface is com-

monly treated with a variety of mold release agents.¹¹ For silicon dioxide templates, self-assembled monolayers of alkyl silanes with fluorocarbon outer tails are widely used,^{12–16} increasing the hydrophobic properties of the treated templates, with water contact angles in the range 90°–110° (Ref. 17) and surface energies around 20 mJ/m².

Diamondlike carbon (DLC) is an attractive option as a base material for NIL templates. DLC films can easily be deposited on Si or quartz substrates by plasma enhanced chemical vapor deposition (PECVD) and they possess excellent mechanical properties, which is particularly important for NIL because of the high mechanical forces applied during imprint.¹⁸ Ramachandran *et al.*¹⁹ successfully demonstrated the use of DLC templates for NIL, achieving good separation from the imprinted resist for the patterning of 1 μm wide lines.

Although the surface energy of as-deposited DLC is relatively low (~40 mJ/m²),²⁰ which makes DLC useful as a material for antiadhesion coatings in many applications,²¹ it is still not low enough for achieving smooth and easy postimprint separation. Thus, an additional surface treatment is required. It has already been demonstrated that *in situ* fluorination of DLC during growth (i.e., adding fluorocarbons to the PECVD gas mixture) significantly lowers its surface energy, resulting in more hydrophobic films compared

^{a)}Electronic mail: sw2128@columbia.edu

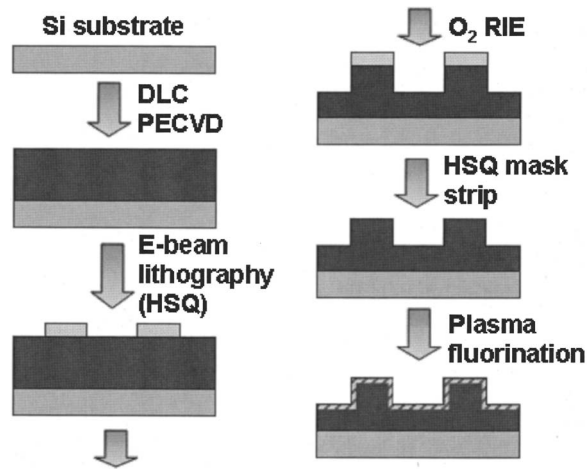


FIG. 1. Schematic process flow of DLC-based NIL template fabrication.

to pure DLC.²² *In situ* fluorinated DLC was reported as an antiadhesion coating for SiO₂ NIL templates²³ with a thickness of 50 nm, and implemented for patterning of features with dimensions of a few hundreds of nanometers.²⁴ Exposing the surface of pure DLC to a fluorocarbon plasma can be used to modify its surface properties as well, significantly lowering the surface energy²⁵ and making its antiadhesion characteristics well suited for nanoimprint application.

In this work we report on the use of a DLC film that undergoes a fluorocarbon-based plasma treatment to lower the surface energy of the DLC. These films are used as templates to pattern ultrasmall (sub-20 nm) features by NIL. Additional applications of fluorocarbon plasma treatment to reduce adhesion are also demonstrated: Direct treatment of nanoimprint resists for use with templates that have no antiadhesion surface treatment, as well as for polymer molds that are used for the preparation of elastomer stamps used in microcontact printing.

II. EXPERIMENT

The process flow of the NIL template fabrication is schematically presented in Fig. 1. DLC films, 100–200 nm thick, were deposited on Si substrates in a parallel plate rf PECVD system. Prior to the deposition, the Si substrates were cleaned in an Ar plasma at 100 mTorr and 125 W for 30 s. Pure cyclohexane was used for the DLC film growth, at a chamber pressure of 100 mTorr, rf power of 200 W, and a temperature of 60 °C. Under these conditions the growth rate of DLC was 3.4 nm/s.

The templates were patterned by electron beam lithography using hydrogen silsequioxane (HSQ) as a negative-tone resist. 20 nm thick HSQ (Fox-12, Dow Corning), diluted in methyl-isobutyl-ketone, was applied to Si/DLC substrates by spin coating. The HSQ was not baked prior to the e-beam exposure, in order to maximize contrast.²⁶ An FEI XL-30 Sirion scanning electron microscope equipped with a Nabity NPGS pattern generator was used for the e-beam patterning. Exposure was done at 30 keV with a probe current of 25 pA for the highest resolution features. The HSQ was developed

in 0.26N TMAH (Microposit LDD-26W), followed by a deionized water rinse. The pattern consisted of features of different sizes and geometries: The finest features were dots with diameters ~10–20 nm, arranged in arrays with interdot spacing in the range 40–200 nm.

Direct patterning of DLC by an inorganic e-beam lithography resist, such as HSQ, followed by O₂ etching provides a simple process flow for DLC-based template fabrication. An Oxford PlasmaLab 80 Plus etch system was used for O₂ plasma etching of the DLC, with a typical chamber pressure of 75 mTorr, gas feed rate of 100 SCCM (SCCM denotes cubic centimeter per minute at STP), and rf power of 50 W. Substrates were typically 12 × 12 mm² in size. The fact that the HSQ mask remains untouched by the oxygen plasma etching allows us to use very thin (down to 20 nm) films of HSQ, in which features with size as small as 10 nm and less can be patterned by e-beam lithography. In this work, the DLC was etched to a depth of 30–50 nm, providing an aspect ratio of 1:2 to 1:3 for the finest features.

DLC surface fluorination was done in an Oxford PlasmaLab 80 Plus etch system. C₄F₈ or CHF₃ gas was used as source material, with the chamber pressure varying in the range 33–88 mTorr, the rf power in the range 100–300 W, and the gas feed rate of 200 SCCM. The typical fluorination time was 30 s. For most of our experiments, standard conditions were chosen as 88 mTorr and 100 W, and these parameters were used for all the plasma fluorination processes mentioned below.

Null (single wavelength, 632.8 nm) ellipsometry (Rudolf El III), tapping mode atomic force microscopy (PSIA XE-100), water and glycerol contact angle measurements, and x-ray photoelectron spectroscopy (XPS) (Kratos Axis Ultra spectrometer with an Al K α 1486 eV monochromatic x-ray source) were used to characterize the physical and the chemical properties of DLC surfaces.

NIL was done using a Nanonex BX-200 nanoimprint system, with polymethyl-methacrylate (PMMA) ($M_w=35$ K) as the imprint resist. The PMMA thickness varied from 50 to 150 nm, and usually was designed to provide a minimal residual layer of 20–30 nm, depending on the featured height on the NIL template and the template geometry. Typically, the imprint was performed at 3.45 MPa, and 180 °C for 5 min.

For the experiments in which we fluorinated the imprint resist, 120 nm of PMMA ($M_w=35$ K) was spun onto Si substrates, followed by nanoimprint with Si/SiO₂ templates without any antiadhesion treatment. The template pattern consisted of arrays of lines with the width from 100 to 200 nm and a height of 100 nm. The same fluorination and imprint conditions described above were used.

PMMA resist films, imprinted on Si substrates and plasma-fluorinated in the same manner, were used as molds for the preparation of microcontact printing stamps from a polydimethylsiloxane (PDMS) elastomer, in order to facilitate the separation between mold and template, which we have found to be somewhat difficult in the case of high-aspect-ratio structures. In this case, the PMMA molds con-

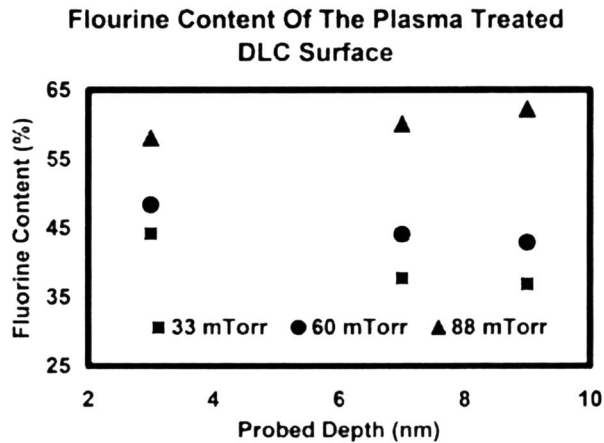


FIG. 2. Average percentage of fluorine in the modified DLC surface as a function of depth for three different chamber pressures, as measured by XPS.

sisted of imprinted channels with a width of $0.5 \mu\text{m}$ and a depth of $5 \mu\text{m}$. PDMS was applied to the surface of the molds and left overnight at the room temperature for complete curing before mechanical separation.

III. RESULTS AND DISCUSSION

Null ellipsometry was used to characterize the DLC films before and after plasma fluorination, providing information about any film thickness change upon the plasma treatment. It was found that for most process conditions, the DLC films thickness either remained unchanged or decreased by a few nanometers probably due to minor etching of the DLC by the plasma under the lower pressure and higher power conditions.²⁷ (For higher chamber pressures, an additional $\sim 3 \text{ nm}$ thick film was detected by ellipsometry.) Atomic force microscopy measurements showed that for bare DLC, as well as for the DLC after O_2 plasma etching and for the DLC after O_2 plasma etching followed by plasma fluorination, the surface roughness did not exceed a rms value of 0.7 nm . The advancing contact angle of water was found to increase from 70° for bare DLC to $\sim 90^\circ$ – 100° upon the plasma fluorination under different conditions for both C_4F_8 and CHF_3 , pointing to a similar chemical content of the modified surface in the two cases. A similar increase from 50° to $\sim 80^\circ$ – 85° was observed for the advancing contact angle of glycerol. No significant change in contact angle was observed after several imprint cycles. XPS analysis of the fluorinated DLC surface detected the presence of a thin fluorine-containing layer near the DLC surface. The thickness of this layer, as calculated from the three different take-off-angle measurements, varied with the processing conditions, and was found to be up to 3 nm for the highest chamber pressure (88 mTorr). The relative concentration of fluorine at different depths was found to depend on the plasma conditions as well (Fig. 2).

Nanoimprint of PMMA with fluorinated DLC templates resulted in easy template-substrate separation, with no PMMA residuals on the templates and high-quality pattern

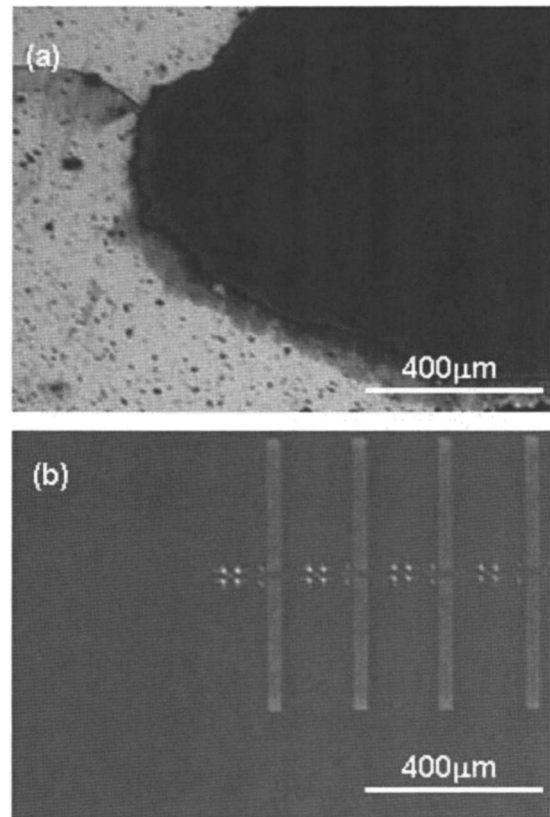


FIG. 3. (a) PMMA resist after imprint using a DLC template on which the fluorinated antiadhesion coating was damaged. The left part of the image shows a large area from which the PMMA resist film was completely detached following separation. (b) The same pattern, imprinted with a perfectly fluorinated DLC template.

transfer to the resist. In contrast, in the case of untreated DLC templates or DLC templates where the coating was damaged (usually by contamination), PMMA tended to adhere to the template. In many cases, the detached PMMA regions were quite extensive and covered significant portions of the template surface (Fig. 3). The plasma fluorination antiadhesion coating was found to be extremely durable, withstanding more than 100 imprint cycles. In the few cases where antiadhesion failure was noted, it was generally due to external factors, such as surface contamination due to the particles and impurities in the air and resist.

Figure 4(a) shows the HSQ pattern on a DLC template. The pattern consists of dots arranged in array of pairs with spacing of 200 nm between the pairs. Figure 4(b) shows a side view of the template after O_2 reactive ion etching into the DLC and HSQ mask strip, resulting in pillars with an aspect ratio of about 1:3. An example of the imprint results is shown in Fig. 5. Circular holes, ~ 10 – 15 nm in diameter, defined by the template structures, are seen in the resist.

Exposure of PMMA resist films to the same fluorocarbon plasma provides a highly hydrophilic PMMA surface, increasing its water contact angle from 75° to 90° . Ellipsometry measurements of PMMA thickness before and after the plasma treatment showed no change in PMMA thickness, and confirmed that the PMMA itself is undamaged by the

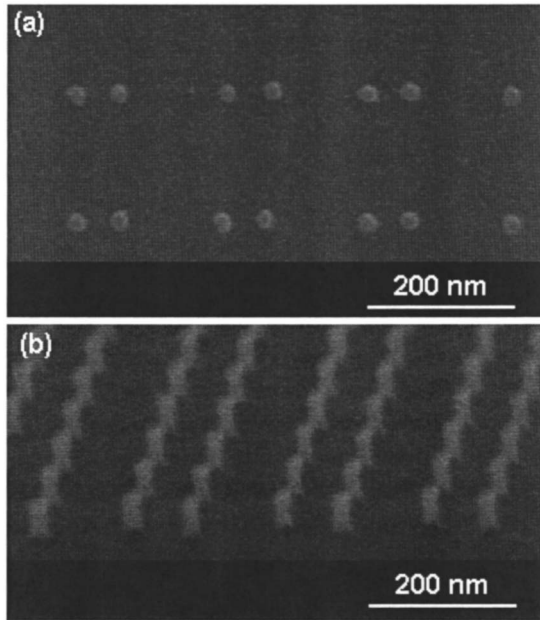


FIG. 4. (a) HSQ mask on DLC surface—top view. (b) Pillars on DLC NIL template, fabricated using the HSQ mask—side view.

plasma process with the parameters described above. Similar to DLC, plasma fluorination of PMMA reduces its surface energy due to the formation of fluorocarbon groups on its surface.²⁸ This enables easy separation from an untreated template after NIL. While imprinting PMMA with an untreated SiO₂ template nearly always leads to separation failure, plasma fluorinated PMMA provided easy and clean template-substrate separation, with a good pattern transfer from the template to PMMA (Fig. 6). Such surface treatment of the nanoimprint resist for each imprinted substrate is certainly less practical than treating the template; however, it could be useful in situations where a low surface energy template is not readily available.

Figure 7 shows an array of PDMS fences, formed by molding in an imprinted PMMA film, which was subjected to plasma fluorination prior to the PDMS application. While

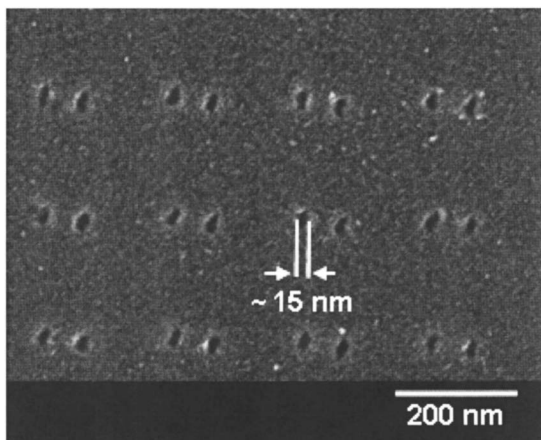


FIG. 5. Array of dots imprinted on PMMA with a fluorinated DLC template.

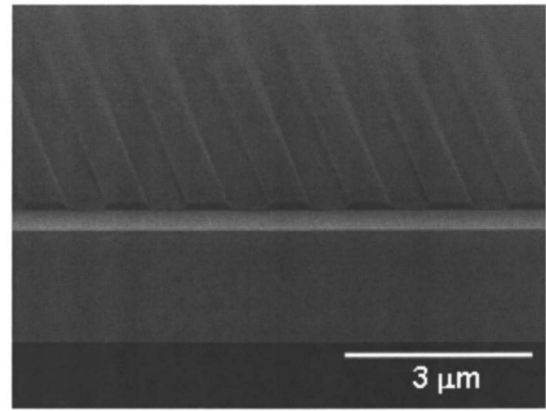


FIG. 6. Cross section of fluorinated PMMA film on Si/SiO₂ substrate, imprinted with untreated SiO₂ template. The pattern consists of lines array with 1.3 μm pitch size.

the removal of PDMS from the mold is sometimes difficult, in case of fluorinated PMMA mold the separation was easy, and high-aspect-ratio (1:10) PDMS structures came out clean and free of defects.

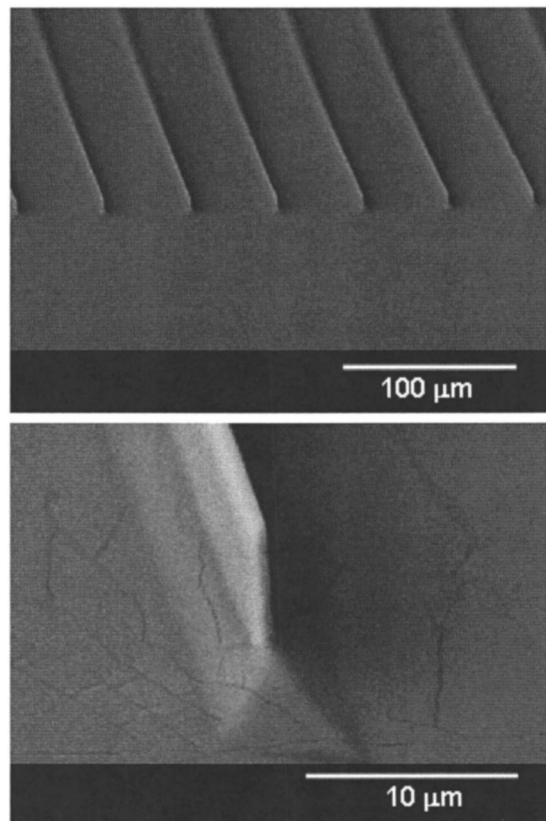


FIG. 7. Array of PDMS fences, formed from a fluorinated PMMA mold. (The cracks visible on the high magnification image are in the 20 nm Au discharge layer, which was sputtered on the top of the surface prior the scanning electron microscopy imaging.)

IV. CONCLUSIONS

We have developed a process for the formation of an ultrathin antiadhesion layer on carbon-based films using a fluorocarbon plasma treatment. Such films are very well suited as templates for nanoimprint lithography—particularly for sub-50 nm features. The process is also applicable to other imprint and molding techniques where a low energy surface is required.

ACKNOWLEDGMENTS

The authors thank Kateryna Artyushkova at the University of New Mexico for assistance with XPS measurements and analysis. This work was supported by the National Institutes of Health through the NIH Roadmap for Medical Research under Award No. PN2EY016586 and by the National Science Foundation under Award No. NSF EF-05-07086. Additional support from the Nanoscale Science and Engineering Initiative of the National Science Foundation under NSF Award No. CHE-0641523 and by the New York State Office of Science, Technology, and Academic Research is also gratefully acknowledged.

¹S. Y. Chou, P. R. Krauss, and P. J. Renstrom, *Appl. Phys. Lett.* **67**, 3114 (1995).

²B. Bilenberg, S. Jacobsen, C. Pastore, T. Nielsen, S. R. Enghoff, C. Jeppesen, A. V. Larsen, and A. Kristensen, *Jpn. J. Appl. Phys., Part 1* **44**, 5506 (2005).

³N. Bogdanski, M. Wissen, S. Möllenbeck, and H.-C. Scheer, *J. Vac. Sci. Technol. B* **24**, 2998 (2006).

⁴L. J. Guo, *J. Phys. D: Appl. Phys.* **37**, R123 (2004).

⁵S. Y. Chou, P. R. Krauss, and P. J. Renstrom, *Science* **272**, 85 (1996).

⁶S. Y. Chou, P. R. Krauss, W. Zhang, L. J. Guo, and L. Zhuang, *J. Vac. Sci. Technol. B* **15**, 2897 (1997).

⁷Y. Nakada, K. Ninomiya, and Y. Takaki, *Jpn. J. Appl. Phys., Part 2* **45**, L1241 (2006).

⁸S. Kiyohara, M. Fujiwara, F. Matsubayashi, and K. Mori, *J. Mater. Sci.: Mater. Electron.* **17**, 199 (2006).

⁹J. Taniguchi, Y. Tokano, I. Miyamoto, M. Komuro, and H. Hiroshima, *Nanotechnology* **13**, 592 (2002).

¹⁰J. Taniguchi, Y. Tokano, I. Miyamoto, M. Komuro, H. Hiroshima, K. Kobayashi, T. Miyazaki, and H. Ohya, *Jpn. J. Appl. Phys., Part 1* **39**, 7070 (2000).

¹¹L. J. Guo, *Adv. Mater. (Weinheim, Ger.)* **19**, 495 (2007).

¹²T. Bailey, B. Choi, J. M. Colburn, M. Meissl, S. Shaya, J. G. Ekerdt, S. V. Sreenivasan, and C. G. Willson, *J. Vac. Sci. Technol. B* **18**, 3572 (2000).

¹³M. Beck, M. Graczyk, I. Maximov, E. L. Sarwe, T. G. I. Ling, M. Keil, and L. Montelius, *Microelectron. Eng.* **61-62**, 441 (2002).

¹⁴M. Colburn *et al.*, *Proc. SPIE* **3676**, 379 (1999).

¹⁵J. J. Dumond, H. Y. Low, and I. Rodriguez, *Nanotechnology* **17**, 1975 (2006).

¹⁶T. Nishino, M. Meguro, K. Nakamae, M. Matsushita, and Y. Ueda, *Langmuir* **15**, 4321 (1999).

¹⁷R. S. Garidel, M. Zelsmann, P. Voisin, N. Rochat, and P. Michallon, *Proc. SPIE* **6517**, 65172 (2007).

¹⁸F. Lazzarino, C. Gourgon, P. Schiavone, and C. Perret, *J. Vac. Sci. Technol. B* **22**, 3318 (2004).

¹⁹S. Ramachandran, L. Tao, T. H. Lee, S. Sant, L. J. Overzet, M. J. Goeckner, M. J. Kim, G. S. Lee, and W. Hu, *J. Vac. Sci. Technol. B* **24**, 2993 (2006).

²⁰M. Grischke, A. Hieke, F. Morgenweck, and H. Dimigen, *Diamond Relat. Mater.* **7**, 454 (1998).

²¹J. Robertson, *Mater. Sci. Eng., R.* **37**, 129 (2002).

²²M. Hakovirta, D. H. Lee, X. M. He, and M. Nastasi, *J. Vac. Sci. Technol. A* **19**, 782 (2001).

²³N. Yamada, K. I. Nakamatsu, K. Kanda, Y. Haruyama, and S. Matsui, *Jpn. J. Appl. Phys., Part 1* **46**, 6373 (2007).

²⁴K. Nakamatsu, N. Yamada, K. Kanda, Y. Haruyama, and S. Matsui, *Jpn. J. Appl. Phys., Part 2* **45**, L954 (2006).

²⁵H. Kasai, M. Kogoma, T. Moriwaki, and S. Okazaki, *J. Phys. D: Appl. Phys.* **19**, L225 (1986).

²⁶W. Henschel, Y. M. Georgiev, and H. Kurz, *J. Vac. Sci. Technol. B* **21**, 2018 (2003).

²⁷M. Schwartzman, A. Mathur, J. Hone, C. Jahnes, and S. J. Wind, *Appl. Phys. Lett.* **93**, 153105 (2008).

²⁸S. Guruvenket, G. R. S. Iyer, L. Shestakova, P. Morgen, N. B. Larsen, and G. M. Rao, *Appl. Surf. Sci.* **254**, 5722 (2008).